Scripta Materialia 138 (2017) 96–99

Contents lists available at ScienceDirect

Scripta Materialia

journal homepage: www.elsevier.com/locate/scriptamat

Regular article

Structural origin of hysteresis for hexagonal $(Mn,Fe)_2(P,Si)$ magneto-caloric compound

Xue-Fei Miao, Hossein Sepehri-Amin *, Kazuhiro Hono [1]

Research Center for Magnetic and Spintronic Materials, National Institute for Materials Science, 1-2-1 Sengen, Tsukuba 305-0047, Japan

ARTICLE INFO

Article history:
Received 15 May 2017
Received in revised form 26 May 2017
Accepted 29 May 2017
Available online xxxx

Keywords:
Magneto-caloric
$(Mn,Fe)_2(P,Si)$
Thermal hysteresis
Phase transformations
Transmission electron microscope

ABSTRACT

We performed in-situ transmission electron microscope observations on the unconventional ferromagnetic transition in hexagonal $(Mn,Fe)_2(P,Si)$ magneto-caloric compounds in order to understand the origin of the large thermal hysteresis that is detrimental to magnetic refrigeration. We find that the ferromagnetic transition is coupled to a martensitic-like transformation. Although crystal structure is the same for both paramagnetic (PM) and ferromagnetic (FM) phases, large lattice distortion occurs during the PM-FM transition, which induces energy barrier of about 13.6 kJ/mol. Supercooling or superheating is therefore needed to overcome the energy barrier, which causes the thermal hysteresis for the ferromagnetic transition.

One of the interesting phenomena accompanied with a magnetic transition is the magneto-caloric effect (MCE), which allows the solid-state refrigeration concept as an energy-efficient and environment-benign alternative to the conventional vapor-compression scheme [1–3]. If the magnetic transition is first order, large magnetization change occurs in a narrow temperature range, leading to a giant MCE. Among a variety of giant MCE materials [4–10], the $(Mn,Fe)_2(P,Si)$-based compounds stand out due to the combination of an outstanding MCE and low material cost [9]. The giant MCE in $(Mn,Fe)_2(P,Si)$ is maximized in the vicinity of a ferromagnetic transition. As revealed by polarized neutron scattering and muon-spin relaxation analysis [11], the ferromagnetic transition in $(Mn,Fe)_2(P,Si)$ is characterized by the extension of magnetic correlations in space and the slowing down of spin fluctuations, which are general features for the conventional ferromagnets. Similar to the conventional ferromagnets, crystal structure is also retained during the ferromagnetic transition for $(Mn,Fe)_2(P,Si)$ compounds. However, in contrast to the conventional ferromagnets, considerable hysteresis is observed in the $(Mn,Fe)_2(P,Si)$ compounds [9,12–14], which significantly reduces the reversibility of the phase transition and hence limits the energy efficiency of magnetic refrigeration [15].

Lots of efforts have been made to investigate the hysteresis in the first-order magneto-caloric materials [16]. For instance, the hysteresis in Heusler alloys is believed to originate from the crystallographic incompatibilities between the martensite and austenite phases [10,17]. For $Gd_5Ge_2Si_2$-based [4], MnAs-based [5], and MnCoGe-based [8] magneto-caloric materials, the hysteresis arises from the structural transformation coupled to the magnetic transition. However, for the $(Mn,Fe)_2(P,Si)$ compounds, the mechanism causing hysteresis remains unknown, because no crystallographic transformation occurs during the ferromagnetic transition, whereas considerable hysteresis is still observed [9,12–14].

Previous studies [9,11–13,18–20] on $(Mn,Fe)_2(P,Si)$ compounds provide mainly atomic-scale and indirect structure information on the ferromagnetic transition, which can hardly elucidate the presence of hysteresis. The aim of this work is to clarify the origin of the large hysteresis in the $(Mn,Fe)_2(P,Si)$ system by observing the microstructure change during the FM-PM transition using in-situ transmission electron microscopy (TEM).

A sample with a nominal composition of $Mn_{1.00}Fe_{1.00}P_{0.62}Si_{0.33}B_{0.05}$ was selected for the present study since it shows considerable hysteresis and its ferromagnetic transition temperature is easy to reach for the in-situ TEM experiments. The sample was prepared from Mn_2P, Fe_3P, Fe, Si and FeB raw materials in an induction melting furnace. The as-cast ingot was sealed under helium atmosphere in a quartz ampoule and then annealed at 1373 K for 5 days before being quenched into water. The actual composition of the as-annealed sample was analyzed using inductively coupled plasma optical emission spectrometry, in good agreement with the nominal one as shown in Table 1.

Powder X-ray diffraction with Cu K_α radiation confirms the formation of the Fe_2P-type hexagonal structure (space group $P\bar{6}2m$) without any detectable impurity phase. Magnetic properties were characterized

* Corresponding author.
E-mail address: h.sepehriamin@nims.go.jp (H. Sepehri-Amin).
[1] Dr. Kazuhiro Hono was an editor of the journal during the review period of the article. To avoid a conflict of interest, Prof. Jeff Th.M. DeHosson acted as editor for this manuscript.

http://dx.doi.org/10.1016/j.scriptamat.2017.05.043
1359-6462/

Table 1
Nominal and measured compositions for the as-annealed $Mn_{1.00}Fe_{1.00}P_{0.62}Si_{0.33}B_{0.05}$ sample.

Elements	Mn	Fe	P	Si	B
Nominal (wt%)	39.30	39.95	13.74	6.63	0.38
Measured (wt%)	39.10_9	39.81_8	13.93_2	6.83_8	0.38_1

using a superconducting quantum interference device vibrating sample magnetometer. Atomic-resolution scanning transmission electron microscopy (STEM) analysis was performed at room temperature on a Titan G2 80–200 microscope. Temperature-dependent TEM observations between 300 and 100 K were carried out on a JEM-2100F microscope. The thin foil for the (S)TEM experiments was lifted out from the as-annealed ingot using a focused ion beam (FIB) system (Helios Nanolab 650, FEI).

Fig. 1(a) shows the temperature-dependent magnetization measured in an applied field of 0.01 T for an as-annealed sample. A large thermal hysteresis of about 35 K suggests a first-order character for the ferromagnetic transition. Intrinsic chemical disorder causes the coexistence of transformed and untransformed phases over the phase transition region. The temperature region where the PM and FM phases coexist upon cooling is highlighted in Fig. 1(a). Fig. 1(b) presents the Arrot plot derived from magnetization isotherms. The *S*-shaped curves reveal relevant high-order terms in the Landau free energy expansion, which proves a first-order character for the ferromagnetic transition [21].

Fig. 2(a) shows a bright-field (BF) TEM image of the as-annealed sample at 300 K. The corresponding energy dispersive spectroscopy (EDS) maps of Mn, Fe, P, and Si obtained from the whole area are presented in Fig. 2(b). No considerable compositional variation is detected within the analysis limit of EDS. Nevertheless, many defects can be clearly observed in the BF TEM image. In order to clarify these defects, atomic resolution high-angle annular dark-field (HAADF) STEM images were taken from the defect regions. Fig. 3(a) is a STEM-HAADF image obtained from region I in Fig. 2(a). The zone axis is identified to be $[1\bar{1}0]$ for region I after comparing the resolved atomic columns with the Fe_2P-type hexagonal structure [11], as illustrated in the inset of Fig. 3(a). The inset of Fig. 3(b) shows a fast Fourier transform (FFT) pattern of the defect area in Fig. 3(a). Atomic configurations for different lattice planes are examined in detail by performing inverse FFT (IFFT) of the corresponding reflections in the FFT image. Fig. 3(b) shows the IFFT image acquired by masking {001} reflections in the FFT image, which represents the atomic configuration of the hexagonal basal plane. Dislocations are clearly visualized in the (001) basal planes. No dislocation is observed for the (110) planes (not shown here). Similar features have also been observed from region II in Fig. 2(a), as presented in Fig. 3(c) and (d). The dislocations are probably associated with the stacking faults of Mn and Fe layers along the hexagonal *c* axis since the sample is quenched after high-temperature annealing.

In-situ TEM observations were performed while the as-annealed sample was thermally cycled between 300 and 100 K. As shown in Fig. 4(a), upon cooling down from 300 K to 260 K, many lenticular-shaped structures appear in the BF-TEM image, which is very similar to a martensitic transformation [22]. Fig. 4(b) shows the SAED obtained from an area containing the lenticular-shaped structure and the original matrix phase, as marked by a circle in Fig. 4(a). Two sets of diffraction patterns were detected, characterized by the same crystal structure but slightly different lattice constants and crystal rotation of about 2°. This is consistent with the thermomagnetic results in Fig. 1(a), indicating the coexistence of FM and PM phases at 260 K. Previous neutron diffraction experiments [12,14] revealed that the PM to FM transition is accompanied by an expansion within the *ab* plane and a contraction along the *c* axis. This allows us to identify the diffraction spots in Fig. 4(b) for the PM and FM phases, respectively. At 260 K, the lattice mismatch between the FM and PM phases along *a* axis (i.e., $\varepsilon_a = \frac{a_{FM}-a_{PM}}{a_{PM}}$), and *c* axis (i.e., $\varepsilon_c = \frac{c_{FM}-c_{PM}}{c_{PM}}$) is 1.3% and −2.1%, respectively.

When the sample was further cooled down to 250 K, the lenticular-shaped regions merged together and propagated along the *c* axis upon further cooling, as shown in Fig. 4(c). Fig. 4(a) and (c) clearly demonstrate the nucleation and growth of the FM phase out of the PM matrix upon cooling. Large amount of strain is accumulated during the transition, which is reflected by the dense strain contour in the BF-TEM images (see Fig. 4(c) and (d)). This eventually causes the fracture of the sample at 100 K, as shown in Fig. 4(d).

The sample was subsequently heated up from 100 K to 300 K. The lenticular-shaped PM phase showed up at 285 K (see Fig. 4(e)), and merged together at 290 K (see Fig. 4(f)). This illustrates the nucleation and growth the PM phase out of the FM matrix upon heating.

In contrast to the conventional ferromagnets without hysteresis, the $(Mn,Fe)_2(P,Si)$ compound shows a large hysteresis during thermal cycling. Hysteresis is essentially a macroscopic manifestation of energy dissipation during the phase transition. Since the ferromagnetic transition in the $(Mn,Fe)_2(P,Si)$ compounds is found to be accompanied by discontinuous changes in lattice constants, the lattice misfit will cause large elastic energy for the nucleation of PM and FM phases. For hexagonal materials, the elastic strain energy (U_e) can be calculated as

$$U_e = \frac{1}{2}\sum_i C_{ii}\varepsilon_{ii}^2 \quad (1)$$

where the C_{ii} is the directional elastic constant, which has recently been obtained from theoretical calculations [23]. As derived from Fig. 4(b), the directional strain values are $\varepsilon_{11} = \varepsilon_{22} = \varepsilon_a = 1.3\%$ and $\varepsilon_{33} = \varepsilon_c =$

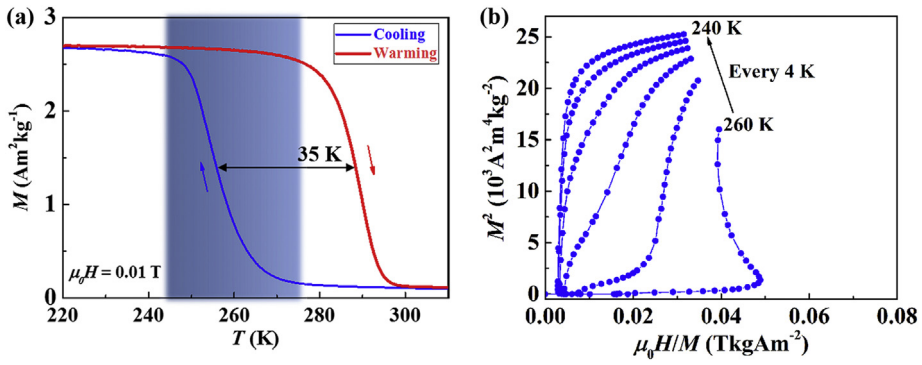

Fig. 1. (a) *M-T* curves and (b) Arrot plots for the as-annealed $Mn_{1.00}Fe_{1.00}P_{0.62}Si_{0.33}B_{0.05}$ sample. The temperature region, where the PM and FM phases coexist, is highlighted in the cooling branch in (a).